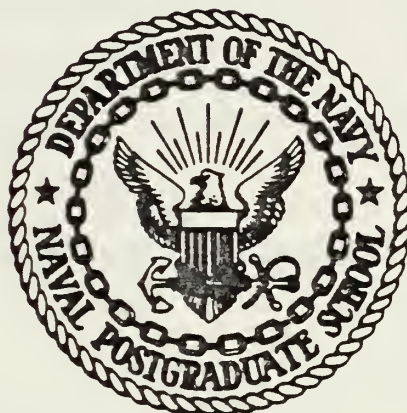


DUDLEY KNOX LIBRARY
NAVAL POSTGRADUATE SCHOOL

NAVAL POSTGRADUATE SCHOOL

Monterey, California



THESIS

GENERATION AND ANALYSIS OF
PARAMETERIZED TERRAIN FOR LAND COMBAT

by

Chung Young Kim

March 1977

Thesis Advisor:

S. H. Parry

Approved for public release; distribution unlimited.

T178062

SECURITY CLASSIFICATION OF THIS PAGE (When Data Entered)

REPORT DOCUMENTATION PAGE		READ INSTRUCTIONS BEFORE COMPLETING FORM
1. REPORT NUMBER	2. GOVT ACCESSION NO.	3. RECIPIENT'S CATALOG NUMBER
4. TITLE (and Subtitle) Generation and Analysis of Parameterized Terrain for Land Combat		5. TYPE OF REPORT & PERIOD COVERED Master's Thesis; March 1977
7. AUTHOR(s) Chung Young Kim		6. PERFORMING ORG. REPORT NUMBER
9. PERFORMING ORGANIZATION NAME AND ADDRESS Naval Postgraduate School Monterey, California 93940		8. CONTRACT OR GRANT NUMBER(s)
11. CONTROLLING OFFICE NAME AND ADDRESS Naval Postgraduate School Monterey, California 93940		10. PROGRAM ELEMENT, PROJECT, TASK AREA & WORK UNIT NUMBERS
14. MONITORING AGENCY NAME & ADDRESS (if different from Controlling Office)		12. REPORT DATE March 1977
		13. NUMBER OF PAGES 59
		15. SECURITY CLASS. (of this report) Unclassified
		15a. DECLASSIFICATION/DOWNGRADING SCHEDULE
16. DISTRIBUTION STATEMENT (of this Report) Approved for public release; distribution unlimited.		
17. DISTRIBUTION STATEMENT (of the abstract entered in Block 20, if different from Report)		
18. SUPPLEMENTARY NOTES		
19. KEY WORDS (Continue on reverse side if necessary and identify by block number) Parametric Terrain		
20. ABSTRACT (Continue on reverse side if necessary and identify by block number) Many current army combat simulation models require digitized terrain inputs for their execution, resulting in a costly and time-consuming operation. A methodology to generate parametric terrain as a function of the number of hill masses and the height, location, spread, and slope of the hills is presented in this paper. Modified Bivariate Normal (MBVN) distribution function and a linear function		

(20. ABSTRACT Continued)

cutting the MBVN function are employed to achieve the terrain representation. Analysis of various terrain parameter values was conducted and the significant trends resulting from the study are described. Finally, recommendations for future enhancement of the model are given.

Approved for public release; distribution unlimited

Generation and Analysis of
Parameterized Terrain for Land Combat

by

Chung Young Kim
Lieutenant Colonel, Korean Army
B.S., ROK Military Academy, 1963

Submitted in partial fulfillment of the
requirements for the degree of

MASTER OF SCIENCE IN OPERATIONS RESEARCH

from the

NAVAL POSTGRADUATE SCHOOL
March 1977

ABSTRACT

Many current army combat simulation models require digitized terrain inputs for their execution, resulting in a costly and time-consuming operation. A methodology to generate parametric terrain as a function of the number of hill masses and the height, location, spread, and slope of the hills is presented in this paper. Modified bivariate normal (MBVN) distribution function and a linear function cutting the MBVN function are employed to achieve the terrain representation. Analysis of various terrain parameter values was conducted and the significant trends resulting from the study are described. Finally, recommendations for future enhancement of the model are given.

TABLE OF CONTENTS

I.	INTRODUCTION -----	7
II.	REPRESENTATION OF TERRAIN -----	9
	A. HIGH RESOLUTION COMBAT MODEL REPRESENTATION -----	9
	B. SYMMETRIC REPRESENTATION -----	10
	C. A NEW REPRESENTATION METHODOLOGY -----	11
III.	THE EXTENDED MODEL -----	12
	A. UNSYMMETRIC TERRAIN -----	12
	B. TERRAIN HEIGHT -----	19
	C. MOVEMENT LINE OF SIGHT -----	20
IV.	TEST AND EVALUATION OF MODEL RESULTS -----	24
	A. DESIGN AND CUTTING ANGLE METHODOLOGY -----	24
	B. OBSERVER-TARGET POSITION -----	27
	C. TARGET MOVEMENT -----	27
	D. TARGET INTERVISIBILITY -----	28
	E. EXPERIMENTAL DESIGN -----	28
	F. ANALYSIS OF RESULTS -----	34
V.	CONCLUSIONS AND RECOMMENDATIONS -----	41
	BIBLIOGRAPHY -----	57
	INITIAL DISTRIBUTION LIST -----	58

LIST OF FIGURES

1.	Unsymmetric Slope Generation -----	12
2.	Cutting Line Determination -----	13
3.	Effect of HI on Hill Shape -----	15
4.	Cutting Direction -----	18
5.	Intersection of Hill Masses -----	19
6.	Intersection of OT Line with Hill Mass -----	21
7.	Cutting Angle and Shape -----	25
8.	Cutting Angle Methodology -----	26
9.	Output Data -----	29
10.	ANOVA Table -----	37
11.	Tilted Method -----	43
12.	Terrain: 1, # of Hills; 18, Average Height; 100, Slope; Down -----	45
13.	Terrain: 2, # of Hills; 18, Average Height; 300, Slope; Up -----	47
14.	Terrain: 2, # of Hills; 12, Average Height; 100, Slope; Up -----	49
15.	Terrain: 3, # of Hills: 6, Average Height; 200, Slope; Side -----	51
16.	Terrain: 3, # of Hills; 6, Average Height; 300, Slope; Side -----	53
17.	Terrain: 1, # of Hills; 12, Average Height; 200, Slope; Both -----	55

I. INTRODUCTION

Many current army combat simulation models require digitized terrain inputs for their execution. This process is very costly and requires a significant amount of computer storage. In addition, computation of line-of-sight and mobility require a great deal of computer running time.

The current methodology utilized to represent terrain is also questionable from a statistical point of view. A Vector Research Incorporated (VRI) study on terrain line of sight, concluded that "... present and past army study results, based on the analysis of combat results on a very limited sample of terrains, may have been determined by the terrain selection process and not by the actual weapon system or force design differences." More specifically it stated the following:

A. "There is extreme sensitivity in combat model results as the scenarios (terrain and movement assumption) are varied, even when variation is within a class of scenarios chosen for their a priori equivalence."

B. "This sensitivity can be slightly reduced, but remains extreme (with probabilities of win estimable only within plus or minus 25%) even when battle results are used to redesign scenarios."¹

¹Farrell, Robert L. and Richard J. Freedman, Investigation of the Variation of Combat Model Predictions with Terrain Line of Sight, Vector Research Incorporated, 1975.

These results imply that sufficient replications of each type of terrain should be run in order to reach a satisfactory statistical level of significance. For VRI's analysis at least fifty replications of each type of terrain were used.

In view of the problems stated above, research was undertaken by Major Christopher Needels² to develop a new methodology for the representation of terrain. In particular, a modified bivariate normal distribution function was utilized to generate hill masses in a wide variety of configurations. Line of sight and movement routines were also developed to evaluate various intervisibility parameters over many terrain configurations for very low cost.

This thesis represents an extension of the models developed by Needels to generalize the terrain generation routines. In particular, methodology was developed to generalize the hill mass generation from symmetric hill shapes to non-symmetric configurations. The methodology developed for this generalization is described in Chapter III.

In order to evaluate the effects of the number of hills, hill height, and slope on various intervisibility parameters, an experiment was designed to measure these effects. A description of the design methodology and results of the analysis are given in Chapter IV. Finally, the conclusions drawn from the current analysis and recommendations for future research are presented in Chapter V.

²Needels, Christopher J., Parameterization of Terrain in Army Combat Analysis, Master's Thesis, Naval Postgraduate School, Monterey, California, 1976.

II. REPRESENTATION OF TERRAIN

A. HIGH RESOLUTION COMBAT MODEL REPRESENTATION

The classic approach to representing terrain in land combat models is to utilize digitized terrain evaluation data from Waterway Experiment Station (WES) for the particular area of interest.

The Dynamic Tactical Simulator (DYNTACS) model serves as a good example of the state of the art in terrain representation and use. DYNTACS is a two-sided dynamic model of battalion level combat representing the detailed interaction of elements in a combined arms environment.

DYNTACS utilizes 100 meter grid squares for which macro-terrain elevations are determined from WES tapes. The simulation divides each grid square diagonally, thus providing a series of adjoining triangular terrain. The entire battlefield, therefore, is represented as a surface of equal size triangles which vary in slope depending on the elevation at their corners.

Needels (pp. 9-10) provides a concise description of the DYNTACS methodology for line of sight calculation as follows.

From the macro-terrain data, line of sight between any two opposing elements is computed. This is accomplished by first computing the angle between the horizontal and a straight line drawn between an observer and target (O-T Line). The program then conducts a search of the terrain along the path of the O-T line to see if any macro-terrain is

higher than the O-T line itself. This is accomplished by comparing the angle of the O-T line with the angle above horizontal of the Observer-Terrain line. If the latter angle is larger, there is no intervisibility. Over the duration of a battle with numerous elements this calculation may be made thousands of times. Consequently, not only is the time to prepare the tapes high, but also the time to compute lines of sight once the terrain is input to the model. Considerable effort by developers and users of this model has been expended to streamline this subroutine.

B. SYMMETRIC REPRESENTATION

The basic models developed by Needels³ (hereafter referred to as SIMTER) which provide the basic foundation for the methodology developed in this thesis are described in this section. The basic motivation for SIMTER was to develop a random terrain representation which could be replicated quickly but at the same time be representative of a particular "type" of terrain. The approach adopted for SIMTER generated a variable number of hill masses. The shape and height of the hills could be varied, but each hill was symmetric, since it was generated directly from the modified bivariate normal (MBVN) density function.

SIMTER has two parts. The first part is the main program which creates terrain and, at the discretion of the user, plots both a three-dimensional drawing and a contour map. Used strictly for terrain generation, it can be used as a preprocessor for other combat models by producing grid points and elevations similar to those provided on computer

³Needels, Parameterization of Terrain in Army Combat Analysis.

tapes by WES. The second part of SIMTER is a movement/line of sight routine which moves a target along specified routes across the generated terrain.

C. A NEW REPRESENTATION METHODOLOGY

The methodology developed in this thesis provides for the generation of hill masses utilizing MBVN density function to represent masses that are not symmetric. This development provides a significant increase in flexibility to represent hill masses more realistically. The mathematical development of this methodology is presented in the next chapter, after which actual results from executing the model are given.

III. THE EXTENDED MODEL

A. UNSYMMETRIC TERRAIN

The unsymmetric slope of terrain can be generated by a cutting method using the MBVN as follows:

$$Z = MH \cdot \text{EXP} \left\{ - \frac{1}{\lambda(1-\rho^2)} \left[\left(\frac{x-\mu_x}{\sigma_x} \right)^2 - 2 \left(\frac{x-\mu_x}{\sigma_x} \right) \left(\frac{y-\mu_y}{\sigma_y} \right) + \left(\frac{y-\mu_y}{\sigma_y} \right)^2 \right] \right\}$$

where MH: maximum height of hill
 Z : height of hill
 μ_x, μ_y : spread of hill
 ρ : ellipse factor of hill

The unsymmetric slope of the hill can be represented by the vertical value of the MBVN subtracted from the vertical value of a linear function as shown in Figure 1 by the value HI.

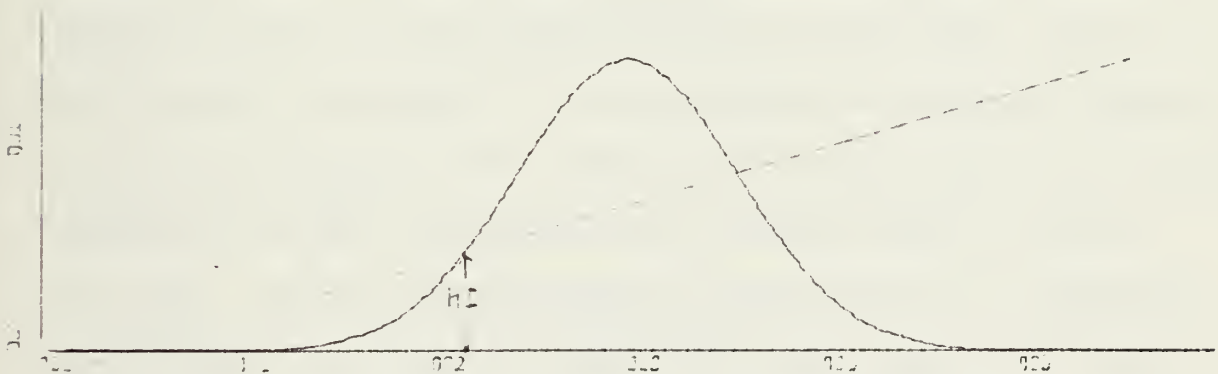


FIGURE 1. UNSYMMETRIC SLOPE GENERATION

Two basic questions must be addressed:

1. Where do we start the cutting of the MBVN function?
2. How do we compute the initial cutting position?

If M is the direction of the cutting line (Line A), then the cutting plane is through the location of the center of the hill (μ_x, μ_y) as shown in Figure 2.

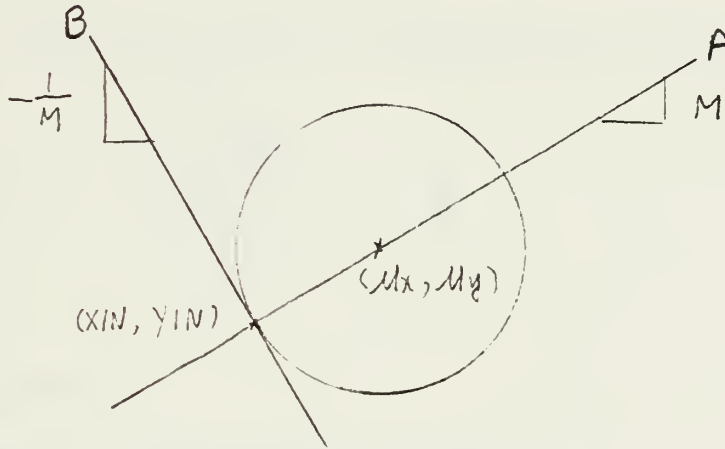


FIGURE 2. CUTTING LINE DETERMINATION

If the initial point of cutting is (x_{IN}, y_{IN}) and HI is height at the initial point, this point is on the cutting plane and also on the MBVN distribution function. Thus, if we consider the graph in two dimensions as shown in Figure 2, Line B is tangent to the circle at the point that the vertical value on the MBVN function is HI and the slope of Line B is $-1/M$. If the initial point of the cutting is (x_{IN}, y_{IN}) this point is on Line B, Line A and the circle at a height HI on the MBVN function. We can compute the initial point (x_{IN}, y_{IN}) as follows.

1. $\rho = 0$ Case

$$HI = MH \cdot \exp \left\{ -\frac{1}{2} \left[\left(\frac{XIN - \mu_x}{\sigma_x} \right)^2 + \left(\frac{YIN - \mu_y}{\sigma_y} \right)^2 \right] \right\} \quad (1)$$

$$-2 \ln(HI/MH) = \left(\frac{XIN - \mu_x}{\sigma_x} \right)^2 + \left(\frac{YIN - \mu_y}{\sigma_y} \right)^2 \quad (2)$$

From (2), the derivative is computed as follows:

$$\frac{dYIN}{dXIN} = - \frac{\left(\frac{XIN - \mu_x}{\sigma_x^2} \right)}{\left(\frac{YIN - \mu_y}{\sigma_y^2} \right)} = - \frac{1}{M} \quad (3)$$

From (2) and (3)

$$XIN = \mu_x \pm \sigma_x \sqrt{\frac{-2 \ln(HI/MH)}{1 + M^2 (\sigma_y/\sigma_x)^2}} \quad (4)$$

$$YIN = \mu_y \pm \sigma_y M \sqrt{\frac{-2 \ln(HI/MH)}{(\sigma_x/\sigma_y)^2 + M^2}} \quad (5)$$

If $\sigma_x = \sigma_y$, then

$$XIN = \mu_x \pm \sigma_x \sqrt{\frac{-2 \ln(HI/MH)}{1 + M^2}} \quad (6)$$

$$YIN = \mu_y \pm \sigma_y M \sqrt{\frac{-2 \ln(HI/MH)}{1 + M^2}} \quad (7)$$

If the hill is cut from left to right and $\sigma_x = \sigma_y$, then

$$XIN = \mu_x - \sigma_x \sqrt{\frac{-2 \ln(HI/MH)}{1 + M^2}} \quad (8)$$

$$YIN = \mu_y - \sigma_y M \sqrt{\frac{-2 \ln(HI/MH)}{1 + M^2}} \quad (9)$$

If the hill is cut from right to left and $\sigma_x = \sigma_y$, then

$$XIN = \mu_x + \sigma_x \sqrt{\frac{-2 \ln(HI/MH)}{1 + M^2}} \quad (10)$$

$$YIN = \mu_y + \sigma_y M \sqrt{\frac{-2 \ln(HI/MH)}{1 + M^2}} \quad (11)$$

Thus, if the direction of cutting and HI are selected, then the starting point can be computed. Care must be taken in the selection of the value of HI. If HI is too small, then the hill will have an unrealistic shape. The value of HI affects the shape of the hill as shown in Figure 3.

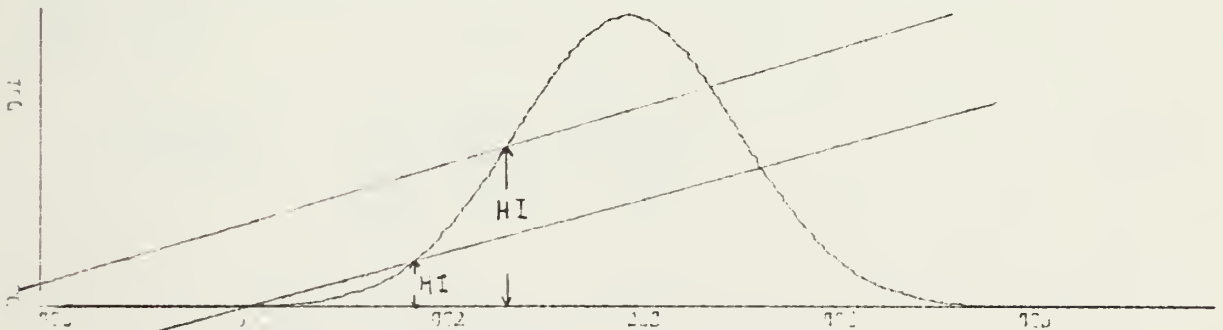


FIGURE 3. EFFECT OF HI ON THE HILL SHAPE

2. 0 < ρ < 1 Case

$$HI = MH * EXP\left\{ - \frac{1}{2(1-\rho^2)} \left[\left(\frac{XIN-\mu_X}{\sigma_X} \right)^2 - 2 \left(\frac{XIN-\mu_X}{\sigma_X} \right) \left(\frac{YIN-\mu_Y}{\sigma_Y} \right) + \left(\frac{YIN-\mu_Y}{\sigma_Y} \right)^2 \right] \right\} \quad (12)$$

$$-2(1-\rho^2) \ln(HI/MH) = \left(\frac{XIN-\mu_X}{\sigma_X} \right)^2 - 2 \left(\frac{XIN-\mu_X}{\sigma_X} \right) \left(\frac{YIN-\mu_Y}{\sigma_Y} \right) + \left(\frac{YIN-\mu_Y}{\sigma_Y} \right)^2 \quad (13)$$

From (13) the derivative is computed as follows:

$$\frac{dYIN}{dXIN} = \frac{- \frac{1}{\sigma_X} \left[\left(\frac{XIN-\mu_X}{\sigma_X} \right) + \left(\frac{YIN-\mu_Y}{\sigma_Y} \right) \right]}{- \frac{1}{\sigma_Y} \left[-\rho \left(\frac{XIN-\mu_X}{\sigma_X} \right) + \left(\frac{YIN-\mu_Y}{\sigma_Y} \right) \right]} = - \frac{1}{M} \quad (14)$$

From (14)

$$\left(\frac{XIN-\mu_X}{\sigma_X} \right) = \frac{\sigma_X + M\rho\sigma_Y}{M\sigma_Y + \rho\sigma_X} \left(\frac{YIN-\mu_Y}{\sigma_Y} \right) \quad (15)$$

$$\text{Let } C = \frac{\sigma_x + M\rho\sigma_y}{M\sigma_y + \rho\sigma_x}$$

From (13), (15) and (16),

$$-2(1 - \rho^2) \ln(HI/MH) = \left(1 - \frac{2\rho}{C} + \frac{1}{C^2}\right) \left(\frac{XIN - \mu_x}{\sigma_x}\right)^2 \quad (17)$$

$$\text{Let } D = 1 - \frac{2\rho}{C} + \frac{1}{C^2} \quad (18)$$

Then

$$XIN = \mu_x \pm \sigma_x \sqrt{\frac{-2(1 - \rho^2) \ln(HI/MH)}{D}} \quad (19)$$

Also, let

$$E = C^2 + 2\rho C + 1 \quad (20)$$

Then,

$$YIN = \mu_y \pm \sigma_y \sqrt{\frac{-2(1 - \rho^2) \ln(HI/MH)}{E}} \quad (21)$$

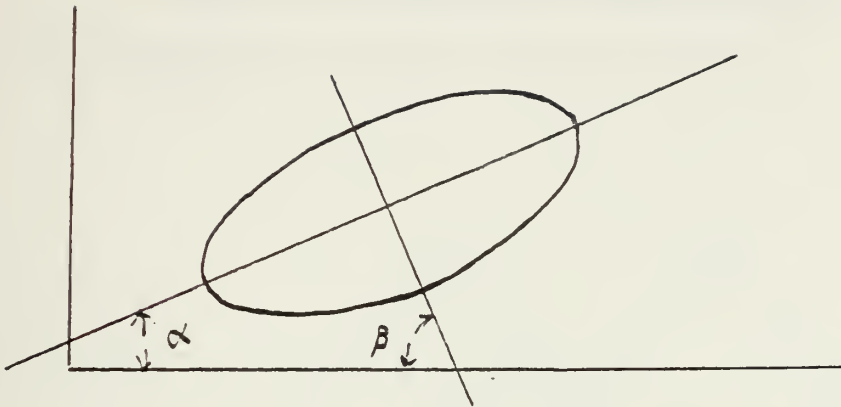


FIGURE 4. CUTTING DIRECTION

If the cutting direction goes through the longer axis as shown in Figure 4, then

$$\cot 2\alpha = \frac{\sigma_x^2 - \sigma_y^2}{-2\rho\sigma_x\sigma_y} \quad (22)$$

The cutting direction, α , is determined by

$$\alpha = \frac{1}{2} \operatorname{arccot} \frac{\sigma_y^2 - \sigma_x^2}{-2\rho\sigma_x\sigma_y} \quad (23)$$

If the cutting direction goes through the shorter axis as shown in Figure 4, then

$$\beta = 90^\circ - \alpha \quad (24)$$

Next, the height of intersecting hill masses must be determined as illustrated in Figure 5.

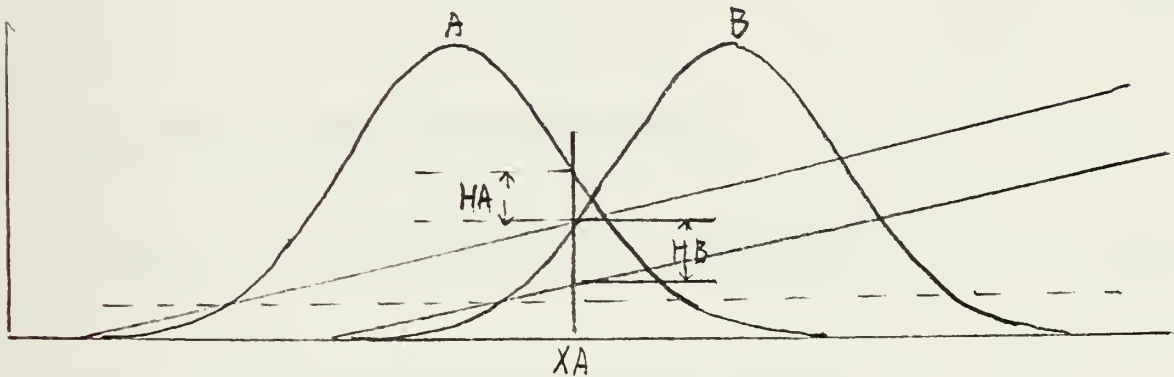


FIGURE 5. INTERSECTING HILL MASSES

HB defines height of hill "B" after cutting.

HA defines height of hill "A" after cutting.

Height of hill "A" is greater than that of hill "B" at the point XA but height of hill "B" is greater than that of hill "A" after cutting. If there is more than one hill located close to each other, those hills must be adjusted by comparing the height after cutting each one. The computation of the height of the terrain at any point is described in the following section.

B. TERRAIN HEIGHT

The height of the hill which is generated by the MBVN distribution corresponds to the height of a hill which is generated by the cutting method. The height of a hill at any point is computed as follows:

The height of the MBVN density function is given by

$$Z = MH \cdot \exp \left\{ - \frac{1}{2(1-\rho^2)} \left[\left(\frac{x-\mu_x}{\sigma_x} \right)^2 - 2\rho \left(\frac{x-\mu_x}{\sigma_x} \right) \left(\frac{y-\mu_y}{\sigma_y} \right) + \left(\frac{y-\mu_y}{\sigma_y} \right)^2 \right] \right\} \quad (25)$$

The height of the linear function is

$$Z_{CUT} = (X - X_{IN}) \tan \theta + (Y - Y_{IN}) \tan \phi \quad (26)$$

where θ = cutting angle of the x-axis
 ϕ = cutting angle of the y-axis.

The height of the hill after cutting is

$$Z_H = \begin{cases} 0 & \text{if } Z < H_I \text{ and } Z_{CUT} < 0 \\ 0 & \text{if } Z < H_I \text{ and } Z_{CUT} > 0 \\ Z - H_I & \text{if } Z > H_I \text{ and } Z_{CUT} > 0 \\ Z - Z_{CUT} - H_I & \text{if } Z > H_I \text{ and } Z_{CUT} > 0 \\ & \text{and } Z > Z_{CUT} + H_I \\ 0 & \text{if } Z > H_I \text{ and } Z_{CUT} > 0 \\ & \text{and } Z < Z_{CUT} + H_I \end{cases}$$

If more than one hill exists at a point on the terrain, the greatest height after cutting is used.

C. MOVEMENT LINE OF SIGHT

The procedure of computing the line-of-sight between any two points on the terrain is described in this section.

If the position of the observer is (OX, OY) and the position of the target is (X, Y) , then the slope of the Observer-Target (O-T) Line is given by

$$ML = \frac{X - OX}{Y - OY} \quad (28)$$

If the intersection point of a hill and the O-T Line is (XI, YI) , then HI and the O-T Line are perpendicular as shown in Figure 6.

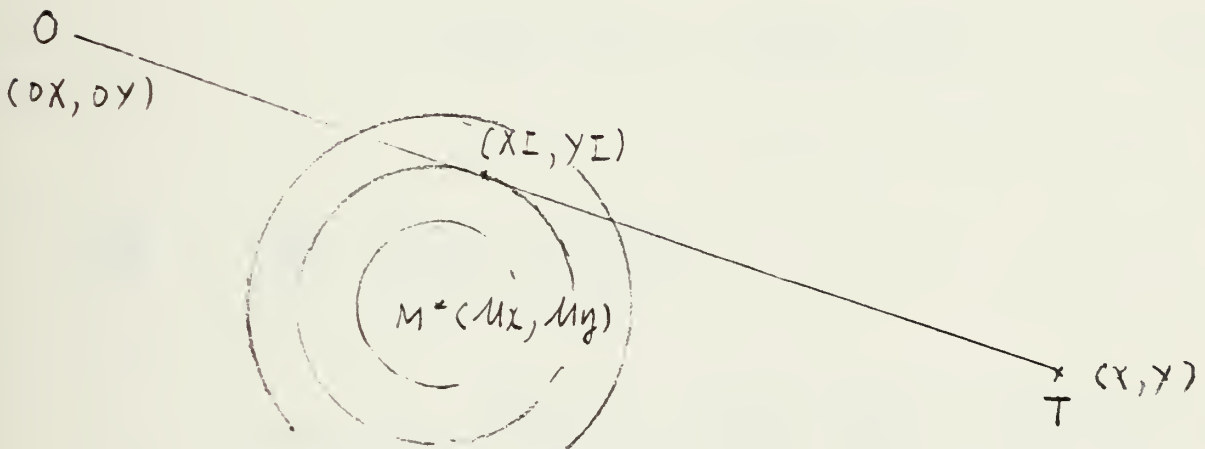


FIGURE 6. INTERSECTION OF O-T LINE WITH HILL MASS

Thus,

$$XI = \frac{ML^2 \cdot OX - ML \cdot OY + \mu_x + ML \cdot \mu_y}{1 + ML^2} \quad (29)$$

$$YI = ML(XI - OX) + OY \quad (30)$$

If there is more than one hill on the O-T Line, the dominant hill (after cutting) is used to compute the percent of the target covered relative to the observer. Target movement along the surface slope of the hill is computed as follows:

$$\begin{aligned}
 ZH = MH * EXP \left\{ - \frac{1}{2(1-\rho^2)} \left[\left(\frac{x-\mu_x}{\sigma_x} \right)^2 - 2\rho \left(\frac{x-\mu_x}{\sigma_x} \right) \left(\frac{y-\mu_y}{\sigma_y} \right) \right. \right. \\
 \left. \left. + \left(\frac{y-\mu_y}{\sigma_y} \right)^2 \right] \right\} \\
 - (X-XIN) \tan \theta - (Y-YIN) \tan \phi \quad (31)
 \end{aligned}$$

$$\begin{aligned}
 \frac{\partial ZH}{\partial x} = \frac{-MH}{1-\rho^2} \left[\left(\frac{x-\mu_x}{\sigma_x} \right) - \frac{\rho(y-\mu_y)}{\sigma_x \sigma_y} \right] \\
 * EXP \left\{ \frac{-1}{2(1-\rho^2)} \left[\left(\frac{x-\mu_x}{\sigma_x} \right)^2 - 2\rho \left(\frac{x-\mu_x}{\sigma_x} \right) \left(\frac{y-\mu_y}{\sigma_y} \right) + \left(\frac{y-\mu_y}{\sigma_y} \right)^2 \right] \right\} - \tan \theta \quad (32)
 \end{aligned}$$

$$\begin{aligned}
 \frac{\partial ZH}{\partial y} = \frac{-MH}{1-\rho^2} \left[\left(\frac{y-\mu_y}{\sigma_y} \right) - \frac{\rho(x-\mu_x)}{\sigma_x \sigma_y} \right] \\
 * EXP \left\{ \frac{-1}{2(1-\rho^2)} \left[\left(\frac{x-\mu_x}{\sigma_x} \right)^2 - 2\rho \left(\frac{x-\mu_x}{\sigma_x} \right) \left(\frac{y-\mu_y}{\sigma_y} \right) + \left(\frac{y-\mu_y}{\sigma_y} \right)^2 \right] \right\} - \tan \phi \quad (33)
 \end{aligned}$$

If DEL is the direction of target movement, then

$$\text{DEL} = \frac{\partial ZH}{\partial x} \cos r + \frac{\partial ZH}{\partial y} \sin r \quad (34)$$

If the speed of the target is constant "V" on the surface, then

$$\text{velocity} = \frac{V}{\sqrt{1 + (\text{DEL})^2}} \quad (35)$$

If the speed of the target is dependent on the slope of the surface, then

$$\text{velocity} = V + W(\text{DEL}) \quad (36)$$

where W is the speed factor of slope.

IV. TEST AND EVALUATION OF MODEL RESULTS

A. DESIGN AND CUTTING ANGLE METHODOLOGY

The methodology for parametrically describing terrain as a function of the number of hills, the center and spread of each hill, and the slope was developed in the previous chapters. In this chapter the effect of the number of hills, height of hills, and the slope on various intervisibility measures is investigated. Three random terrains were generated (with each terrain having six, twelve, and eighteen hills) resulting in nine basic terrain configurations. For each configuration three average hill heights (100, 200, and 300 meters) were utilized.

Finally, for each of the 27 resulting configurations, four slope cutting methods were used as follows:

1. Down slope-cut from observer side to target side.
2. Side slope-cut from right to left as viewed from the target.
3. Up slope - cut from target side to observer side.
4. Both slope-symmetric slope as viewed from any position.

A total of 108 unique terrain configurations were generated for the investigation. For each of the configurations, the mean and standard deviation describing the center and spread of each hill is specified. In addition, the cutting angle for determining slope must also be specified.

If the cutting angle is constant, then the hill can be described as follows:

$$\text{HILL} = F(\text{Peak, Position, Standard Deviation, Slope})$$

In the constant cutting angle case, only the slope is variable, with peak, standard deviation, and position constant. In other words, if the slope varies in Figure 7, the standard deviation of the resulting distribution also varies.

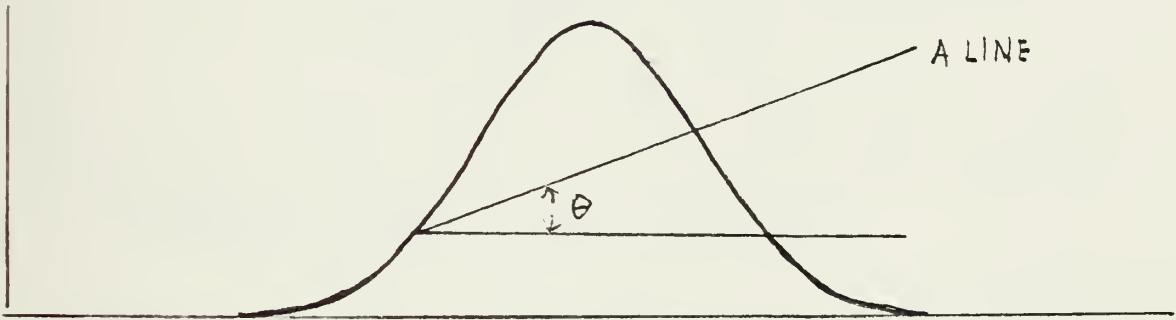


FIGURE 7. CUTTING ANGLE AND SLOPE

The objective of the methodology is to maintain a constant standard deviation of the distribution function resulting from each cutting angle, so that only the slope of the hill varies. Otherwise the determination of how slope affects the intervisibility parameters would not be possible, since it would be confound with the standard deviation (spread) of the hills.

The problem, therefore, was to determine a method to use various cutting angles and maintain a constant standard deviation. After extensive investigations into various approaches to this problem, no method was found which would mathematically guarantee a constant standard deviation. The method shown in Figure 8 was adapted as the best approximation method available.

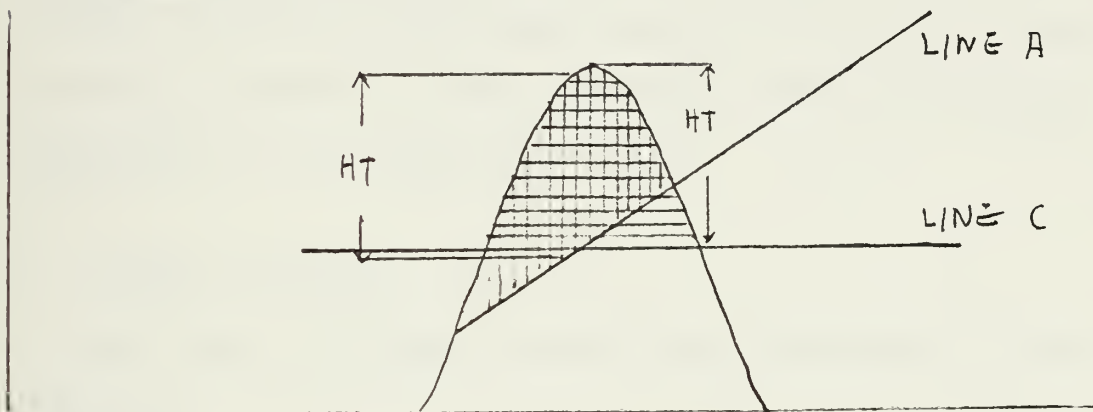


FIGURE 8. CUTTING ANGLE METHODOLOGY

In Figure 8, HT is the maximum height of the hill after cutting with Line A. Note that the cutting angle is now specified in reference to the center line of the original bivariate normal hill mass distribution. In order to generate a symmetric hill mass with approximately the same standard deviation (Line C) the cut is made maintaining a constant maximum height, HT, as in Figure 8.

Several test runs made using this methodology indicated that the resulting standard deviations were very nearly equal for cutting angles. However, very little change in slope results for cutting angles greater than twenty degrees.

B. OBSERVER-TARGET POSITIONS

For each terrain an observer position and initial target position were selected. Two routes from the target to the observer position were selected in accordance with accepted tactics of advance routes. Selected terrains indicating the observer-target position and selected routes are shown in Figures 12 through 17. In order to assure that the "number of hills" factor was properly analyzed, the same routes of approach on each generated terrain were used, independent of the number of hills. ✓

C. TARGET MOVEMENT

Two cases of target movement were considered in the analysis.

1. Constant Speed

The target moves along the route at a constant speed of six meters per second, independent of hill slopes. The constant speed runs serve as the base case for measurement of the percent of time intervisible along the route.

2. Variable Speed

The speed of the target is a function of the terrain slope being traversed. The speed of the vehicle is computed by the relationship as follows:

$$\text{velocity} = 6.0 + 4.0(\text{slope})$$

This slope is the directional derivative value at the instantaneous target position on the hill.

D. TARGET INTERVISIBILITY

Five dependent variables describing target intervisibility are computed for each advance route as follows:

1. Percent of time intervisible along the route,
2. The number of intervisibility segments along the route,
3. The average intervisibility segment length,
4. The average intervisibility segment time, and
5. The total length of intervisibility over the route.

Intervisibility parameters are computed by utilizing the line of sight algorithm at fixed time intervals, TL, during the movement run. For this analysis, TL was set equal to one second. A sample output for one compute movement trace is given in Figure 9.

E. EXPERIMENTAL DESIGN

The objective of the analysis is to determine the effects of the number of hills (A), the height of hills (B) and the slope of the hills (R) on target intervisibility. To accomplish this objective, an experiment was designed as described by the following design matrix.

# of Hills	Height	SLOPE			
		Down	Side	Up	Both
6	100				
	200				
	300				
12	100				
	200				
	300				
18	100				
	200				
	300				

FIGURE 9. OUTPUT OF DATA

Definition of Variables

N	Number of hills
XMEL,YMEL	Spread of hills
HITE	Maximum height of hill
RUFY,RUFY,RUFY	Different amount of the spread and height among hills
INCX,INCY	Grid increment for the terrain matrix
XMAP,YMAP	Size of the grid system in meters
XGRID,YGRID	Center position of hill
HIGHT	Maximum height of hill in modified bivariate normal distribution
XSTD,YSTD	Spread of hill (standard deviation)
XSLOP,YSLOP	Cutting angle
DIRECTION	Cutting direction
XINIT,YINIT	Initial position of cutting plane
HEIGHT	Height of hill at the center position on MBVN after cutting
RX,RY	Coordinates of approaching route of target
TIME	Movement time
MAP COORDINATES	Target position at given time
ELEVATION	Target elevation on the terrain
SPEED	Velocity on the terrain at the given time
VISIBLE	1 means visible and 0 means invisible
HLIN	The different height of O-T line at the maximum height of surface of the terrain on the O-T line, and the lower height between observer and target

DZ Maximum height of surface of the terrain on the
 O-T line

KL The hill which is maximum height between the
 observer and target

DLIN Difference maximum height of surface between
 observer and target, and lower height between
 observer and target.

FIGURE 9 CONTINUED

27C88 664283 28C943 816756

N MELX MELY HITE RUFY RUFF
12 400.000 400.000 450.000 20.000 40.000

INCX INCY XMAP YMAP
100 100 6000.000 3000.000

XGRID YGRID FIGHT XSTD YSTD XSLOP YSLOP
1192.582 1176.702 416.293 388.947 388.947 0.0
3724.886 1833.078 447.019 383.900 383.900 0.0
156.201 541.604 432.489 393.837 393.837 0.0
3264.078 741.448 434.652 399.939 399.939 0.0
1355.822 2513.279 449.548 383.576 383.576 0.0
1304.107 287.566 478.353 390.668 390.668 0.0
5133.679 2917.683 464.687 410.295 410.295 0.0
1740.507 2492.071 535.775 394.231 394.231 0.0
2420.586 1245.736 391.053 359.226 359.226 0.0
2517.937 92.407 424.358 402.920 402.920 0.0
1344.937 1868.407 440.643 371.290 371.290 0.0
2362.507 1315.154

CIRECTICN XINIT YINIT HIGHT RX C RY C
1.571 1870.249 1176.698 214.112 5133.0 2917.0
1.571 4401.560 1833.074 245.705 3368.0 2433.0
1.571 3965.833 741.444 227.473 1740.0 2492.0
1.571 2032.558 2513.276 226.616 1192.0 1176.0
1.571 1000.187 687.562 248.222 1700.0 1900.0
1.571 5861.375 2917.678 271.878 1700.0
1.571 2425.952 2492.067 249.386
1.571 4135.721 1245.732 324.231
1.571 3176.988 92.748 205.084
1.571 2049.166 1868.403 215.660
1.571 3015.840 1315.154 245.690

FIGURE 9 CONTINUED

CBSERVER COORDINATES
 304.90000 667.56600 272.08965

TIME	MAP COORDINATES	ELEVATION	SPEED	VISIBLE	HL IN	DZ	KL	DLIN	TOTAL LENGTH	PER CENT INTERVISBLE	TOTAL LENGTH	TOTAL INTERVISBLE	VISBLE TIME
1	5133.000	2917.000	0.0	1	18.281	215.733	1	-33.784	3158.000	0.481	6648.000	3158.000	533
2	5128.202	2915.684	4.976	1	19.355	215.745	1	-32.437					
3	5123.350	2914.354	5.031	1	20.497	215.764	1	-31.006					
4	708.578	904.812	2.185	1	130.413	0.0	1	-141.676					
5	706.676	903.745	2.180	1	129.345	0.0	1	-142.741					
6	704.779	902.681	2.175	1	128.284	0.0	1	-143.805					
7	702.887	901.615	2.170	1	127.215	0.0	1	-144.870					
8	700.595	900.560	2.165	1	126.154	0.0	1	-145.935					
INTERVISIBILITY SEGMENT LENGTHS													
	INTERVISIBILITY	SEGMENT LENGTHS	TIME										
	1	342.000	57										
	2	618.000	103										
	3	612.000	102										
	4	444.000	74										
	5	1182.000	197										
DISTANCE UNCOVERED	DISTANCE COVERED	TOTAL DISTANCE	AVG DISTANCE INTERVISBLE	PER CENT INTERVISBLE	TOTAL LENGTH								
1182.000	5466.000	5463.867	639.600	0.481	6648.000								

The appropriate linear model is as follows:

$$Y_{ijk} = \mu + A_i + B_j + R_k + AB_{ij} + AR_{ik} + BR_{jk} + ABR_{ijk} + \epsilon_{ijkl}$$

where

Y_{ijkl} = intervisibility dependent variable measure

μ = grand mean of the population

A = number of hills, where

i = 1-6 hills
2-12 hills
3-18 hills

B = average height of hills, where

j = 1-100 meters
2-200 meters
3-300 meters

R = direction of slope of hills, where

k = 1-down slope
2-side slope
3-up slope
4-both (symmetric)

Within each cell of the matrix, there are six replications consisting of two routes on each of the three basic terrain configurations.

For the first treatment levels of slope defined above, a cutting angle of fifteen degrees was used, the symmetric case was generated with a cutting angle of zero degrees using the methodology previously described. Four analyses were conducted as representative of the large number of possible situations. The measurements selected were

1. Percent of time intervisible for constant speed and for variable speed, and
2. Number of intervisibility segments for constant speed and for variable speed.

The results for each selected analysis are described in the following section.

F. ANALYSIS OF RESULTS

1. Percentage of Intervisibility Time

a. Constant Speed

($x^{1/8}$ Transgeneration Data)

SUMMARY TABLE - ANOVA

Source	DF	SS	MS	F Ratio
# of hills A	2	0.0437	0.0218	23.6417
height of hill B	2	0.0117	0.0058	6.3209
slope of hill R	3	0.0387	0.0129	13.962
AB interaction	4	0.0006	0.0081	0.1527
AR interaction	6	0.0026	0.0004	0.4759
BR interaction	6	0.0016	0.00027	0.2943
ABR interaction	12	0.0012	0.0001	0.1114
Error	179	0.1655	0.0009	

Each of the three main effects above are significant at the 0.01 level, but no interaction terms are significant.

The following table gives the mean and standard deviation for each treatment level of slope.

<u>Slope</u>	<u>Mean</u>	<u>Std. Dev.</u>
down	0.6130	0.1539
side	0.5214	0.1701
up	0.6926	0.1629
both	0.5573	0.1595

Note that the up slope has the greatest percentage of inter-visibility time; down slope, both, and side slope following in that order.

The following table gives the mean and standard deviation for the treatment levels of number of hills and height of hills for the constant speed case.

<u># of Hills</u>	<u>Mean</u>	<u>Standard Deviation</u>
6	0.6976	0.1620
12	0.5462	0.1620
18	0.5272	0.1490

<u>Height of Hill</u>	<u>Mean</u>	<u>Standard Deviation</u>
100	0.6475	0.1775
200	0.5844	0.1684
300	0.5556	0.1628

b. Speed which Depends on Slope

($x^{3/8}$ Transgeneration Data)

SUMMARY TABLE - ANOVA

Source	DF	SS	MS	F Ratio
# of hills A	2	0.5152	0.2576	34.286
Height of hill B	2	0.2041	0.1020	13.582
Slope of hill R	3	0.3830	0.1277	16.991
AB interaction	4	0.0033	0.0008	0.1090
AR interaction	6	0.0381	0.0064	0.8450
BR interaction	6	0.0165	0.0028	0.3670
ABR interaction	12	0.0091	0.0008	0.1000
Error	179	1.3449	0.0075	

Each of the three main effects above are significant at the 0.01 level, but no interaction terms are significant.

c. Constant and Dependent Speed.

The ANOVA for comparing constant and dependent speed is given in Figure 10. The treatment level data is as follows:

	Mean	Standard Deviation
Constant Speed	0.569	0.1732
Dependent Speed	0.5393	0.1921

A 4-WAY ANCOVA
 FILE NCNAME (CREATION DATE = 03/07/77)
 * * * * * A N A L Y S I S O F V A R I A N C E * * * * *
 BY P E R V I S P E R C E N T A G E O F I N T E R V I S I B I L I T Y
 H I L L N U M B E R O F H I L L
 F I G H T M A X I M U M H I G H T O F H I L L
 S L C P E S L O P E O F H I L L
 S P E E D V E L O C I T Y O F T A R G E T
 *

SOURCE OF VARIATION	SUM OF SQUARES	DF	MEAN SQUARE	F	SIGNIF CF F
MAIN EFFECTS					
HILL	4.848	7	0.693	30.283	0.001
HIGHT	2.005	2	1.003	43.836	0.001
SLCPE	0.770	2	0.385	16.827	0.001
SPEED	1.806	2	0.903	39.474	0.001
	0.243	1	0.243	10.609	0.002
2-WAY INTERACTIONS					
HILL HIGHT	0.354	18	0.020	0.860	0.999
HILL SLOPE	0.025	4	0.006	0.275	0.955
HILL SPEED	0.117	4	0.029	1.283	0.276
HIGHT SLOPE	0.021	2	0.010	0.450	0.555
HIGHT SPEED	0.145	2	0.036	1.580	0.175
SLOPE SPEED	0.028	2	0.014	0.619	0.999
	0.021	2	0.010	0.458	0.555
3-WAY INTERACTIONS					
HILL HIGHT SLOPE	0.052	20	0.003	0.115	0.999
HILL HIGHT SPEED	0.044	8	0.006	0.242	0.955
HILL SLOPE SPEED	0.001	4	0.000	0.009	0.955
HIGHT SLOPE SPEED	0.006	4	0.002	0.068	0.999
	0.001	4	0.000	0.014	0.955
4-WAY INTERACTIONS					
HILL HIGHT SLOPE SPEED	0.000	8	0.000	0.001	0.955
	0.000	8	0.000	0.000	0.955
EXPLAINED	5.255	53	0.099	4.335	0.001
RESIDUAL	6.129	268	0.023		
TOTAL	11.384	321	0.035		

FIGURE 10. ANOVA TABLE
 430 CASES WERE PROCESSED.
 108 CASES (25.1 PCT) WERE MISSING.

2. Number of Intervisibility Segments

a. Constant Speed

SUMMARY TABLE - ANOVA

($X^{1/2}$ Transgeneration Data)

Source	DF	SS	MS	F-Ratio
# of hill A	2	8.3415	4.1708	82.281
Height of hill B	2	0.2402	0.1201	2.369
Slope of hill R	3	2.7278	0.9093	17.938
AB interaction	4	0.0659	0.0165	0.3255
AR interaction	6	0.2686	0.0448	0.8838
ABR interaction	12	0.1389	0.0116	0.2288
Error	179	9.0475	0.5056	

From the ANOVA, the number of hills and slope are significant at the 0.01 level, but the height of hills is not significant.

b. Dependent Speed

SUMMARY TABLE - ANOVA

(X^{1/2} Transgeneration Data)

Source	DF	SS	MS	F-Ratio
# of hill A	2	8.2224	4.1112	79.337
Height of hill B	2	0.2561	0.1281	2.4272
Slope of hill R	3	2.6384	0.8795	16.972
AB interaction	4	0.06446	0.01611	0.311
AR interaction	6	0.2905	0.0484	0.934
ABR interaction	12	0.1289	0.0107	0.2065
Error	179	9.2756	0.0518	0.2065

The results of the dependent speed case are analogous to those of the constant speed case. That is, the number of hills and slope of hills are significant, but the height of hills is not significant.

The mean and standard deviation of the treatment levels are given below.

SLOPE	MEAN		STD DEV	
	CONST	DEP	CONST	DEP
DOWN	4.2075	4.2075	1.04444	1.0444
SIDE	4.1852	4.1852	1.1339	1.1339
UP	3.3148	3.3333	1.1947	1.2131
BOTH	4.4259	4.4259	1.3818	1.3818

# OF HILL	MEAN		STD DEV	
	CONST	DEP	CONST	DEP
6	4.930	3.038	1.1871	0.7166
12	4.139	4.139	1.039	1.0388
18	3.042	4.931	0.7207	1.1788

HEIGHT OF HILL	MEAN		STD DEV	
	CONST	DEP	CONST	DEP
100	3.875	3.875	1.393	1.393
200	4.069	4.069	1.191	1.191
300	4.155	4.169	1.191	1.195

V. CONCLUSION AND RECOMMENDATION

Terrain is one of the key factors in the analysis of land combat. Thus, the representation of terrain in a land combat model is a critical factor in the model design. High resolution combat models typically employ actual terrain data to describe the terrain environment. This approach, although realistic for the specific terrain being represented, is very costly and time consuming to implement.

The goal of the research by Needels and this thesis is to provide a parametric representation of terrain usable either as input to a high resolution combat model or as a "stand-alone" model to investigate intervisibility segment length parameters. In particular, the current model describes the terrain as a function of the number of hill masses, the height of the hills, the position and spread of the hills, and the slope.

A MBVN distribution function and a linear function cutting the MBVN function are employed to achieve the terrain representation. The terrains given in Figures 12 through 17 illustrate the flexibility of the model. In fact, with appropriate selection of the input parameters (given in Figure 9) any desired terrain may be generated.

The results of the analysis described in Chapter IV indicate that slope is highly significant in the resulting values of intervisibility parameters. Some of the trends

noted from the results given in Chapter IV are described below.

1. An up slope (cut from target side to observer side) resulted in the largest value of percent intervisibility time.
2. Increases in the number and height of hills resulted in decreases in the percent intervisibility time.
3. Speed dependent on terrain slope resulted in a slight reduction in percent intervisibility time from the constant speed case.

The analysis of the hypothetical data described in Chapter IV serves to illustrate the potential utilization of the model. The trends indicated from the analysis are appropriate for the selected terrains and conditions, but should not be construed as generalized results.

An alternate method (tilted method) for generating unsymmetric terrain outlined below is suggested as an area for future enhancement of the model. Given a MBVN density function centered at Y in Figure 11, define θ as the tilted angle, assuming $\rho = 0$. The height of the density function is Z2 at Y2 and is given by

$$Z2 = MH * \exp\left\{-\frac{1}{2} \left[\left(\frac{x - \mu_x}{\sigma_x}\right)^2 + \left(\frac{y - \mu_y}{\sigma_y}\right)^2 \right]\right\} \quad (38)$$

and

$$\frac{Z2}{Y2 - Y} = \tan \left[\frac{\pi}{2} - \theta \right] \quad (39)$$

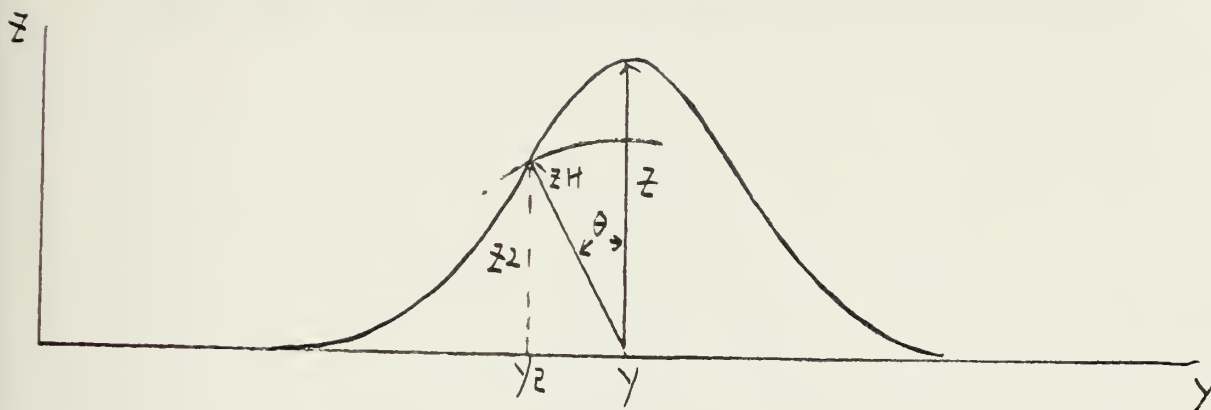


FIGURE 11 TILTED METHOD

From 38 and 39,

$$MH \cdot \exp \left\{ -\frac{1}{2} \left[\left(\frac{x - \mu_x}{\sigma_x} \right)^2 + \left(\frac{y - \mu_y}{\sigma_y} \right)^2 \right] \right\} = (y - y_2) \tan \left(\frac{\pi}{2} - \theta \right) \quad (40)$$

For a specified value of x and y , the value of y_2 can be computed using the golden section method. The tilted height, ZH , can then be computed as follows:

$$ZH = \frac{y - y_2}{\sin \theta} \quad (41)$$

Additional investigation of this method is required before implementation in the model.

In conclusion, a model has been developed and exercised which provides a potentially valuable tool for efficient analysis of various terrain effects in the land combat environment. The intervisibility parameters output from the model can serve as critical inputs to land combat models

for evaluating such things as the contribution of mobility, agibility, and firepower to battlefield survivability.

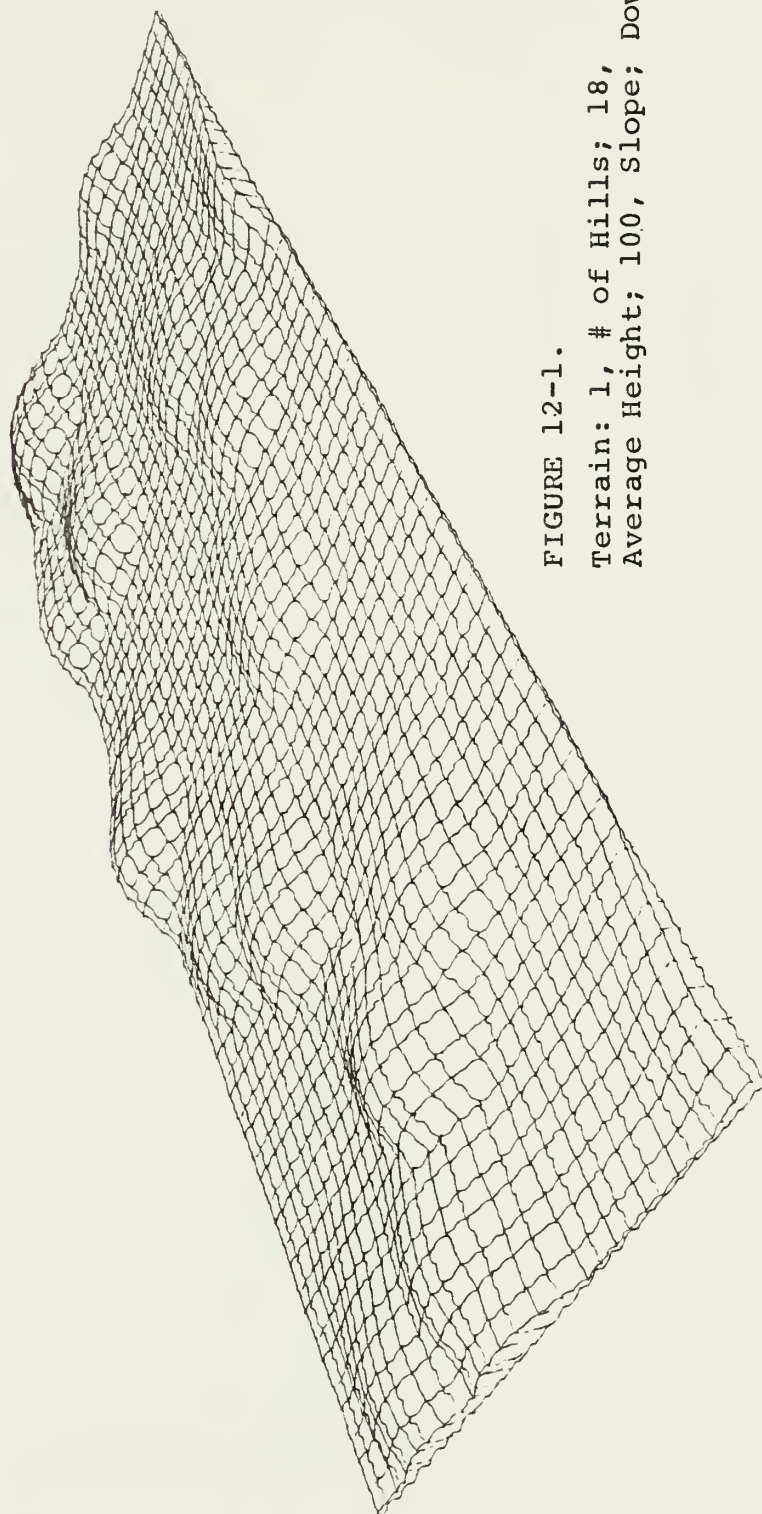


FIGURE 12-1.

Terrain: 1, # of Hills; 18,
Average Height; 100, Slope; Down

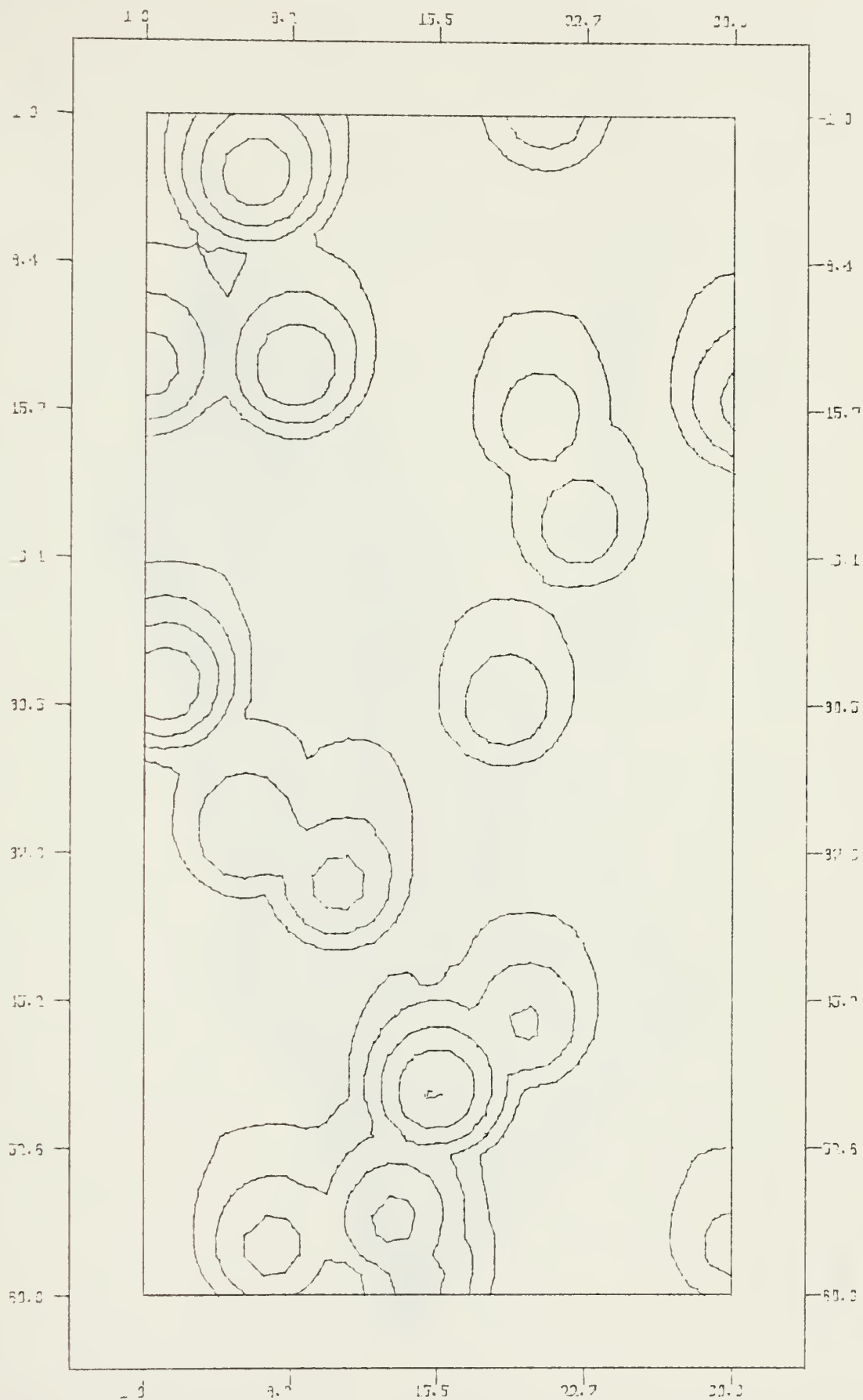


FIGURE 12-2. Terrain: 1, # of Hills; 18, Average Height; 100, Slope; Down

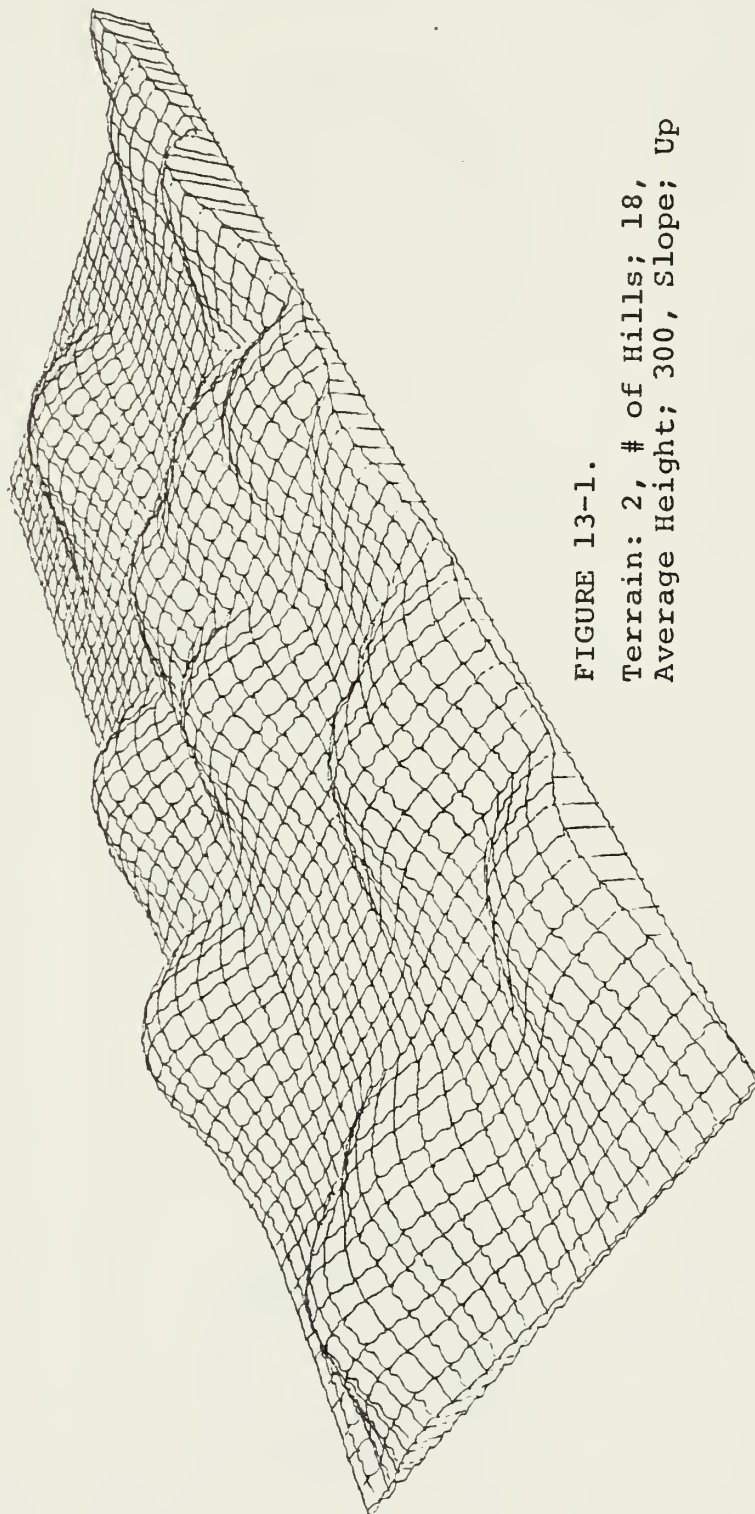


FIGURE 13-1.
Terrain: 2, # of Hills; 18,
Average Height; 300, Slope; Up

TERRAIN

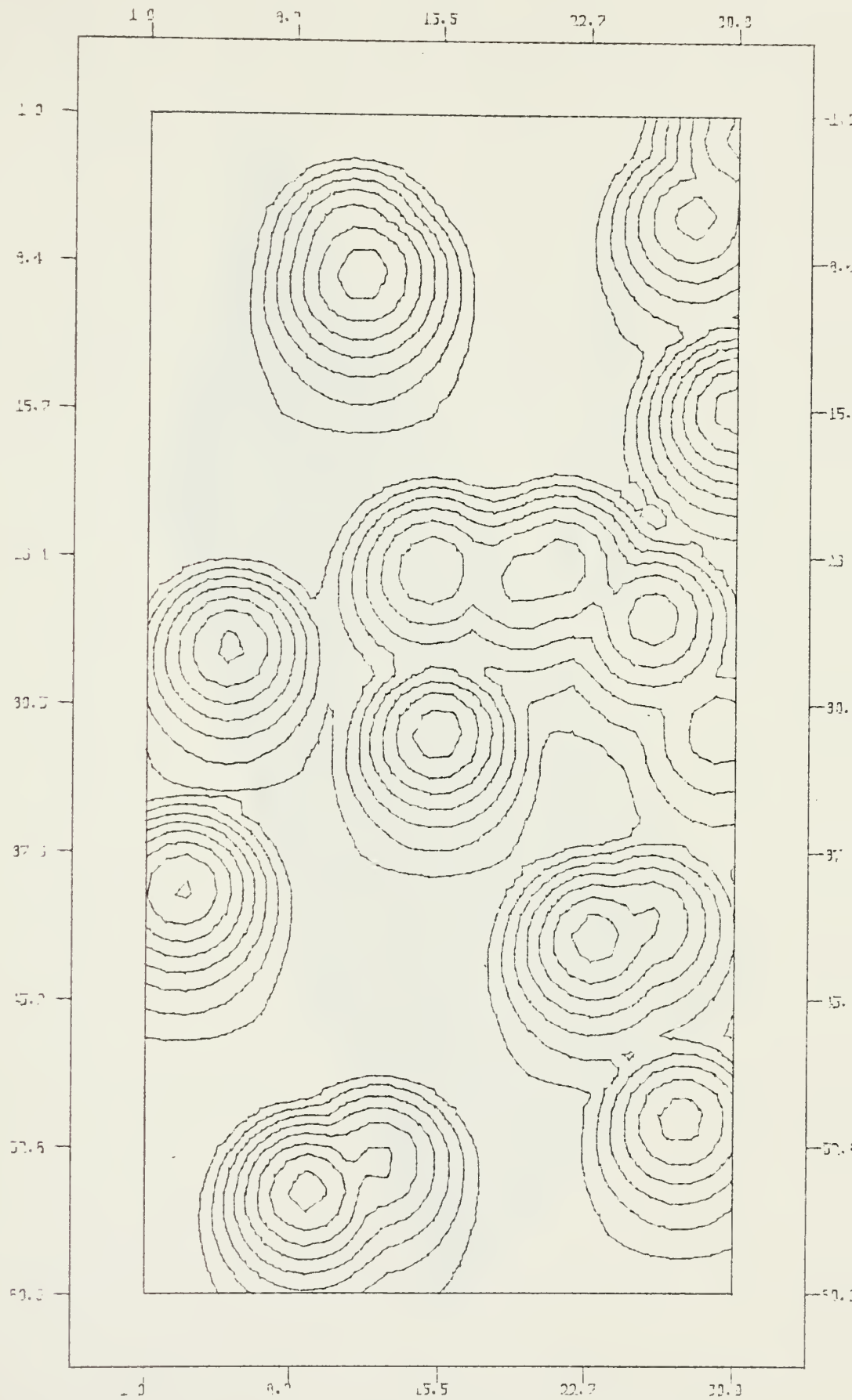


FIGURE 13-2. Terrain: 2, # of Hills; 18, Average Height; 300, Slope; -Up

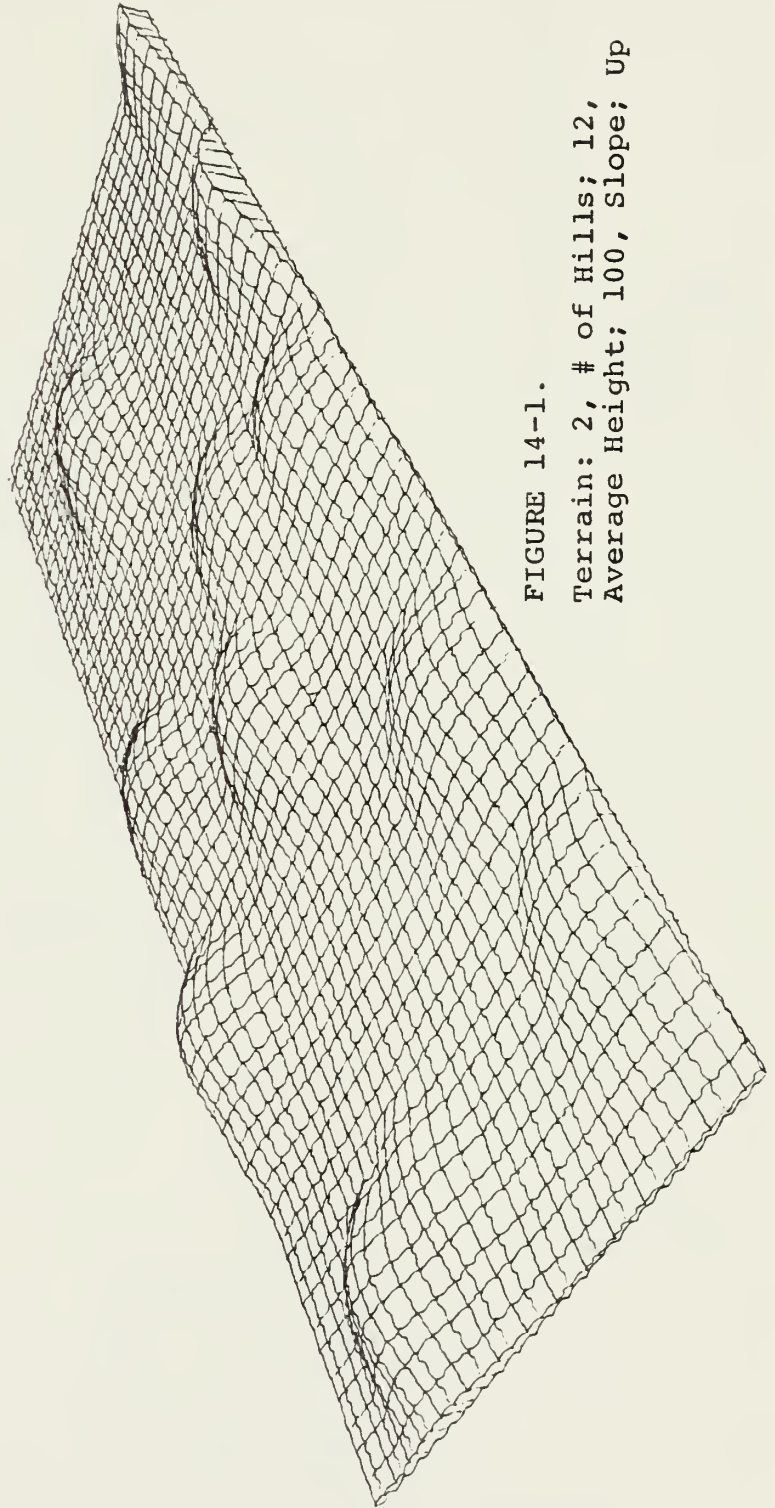


FIGURE 14-1.

Terrain: 2, # of Hills; 12,
Average Height; 100, Slope; Up

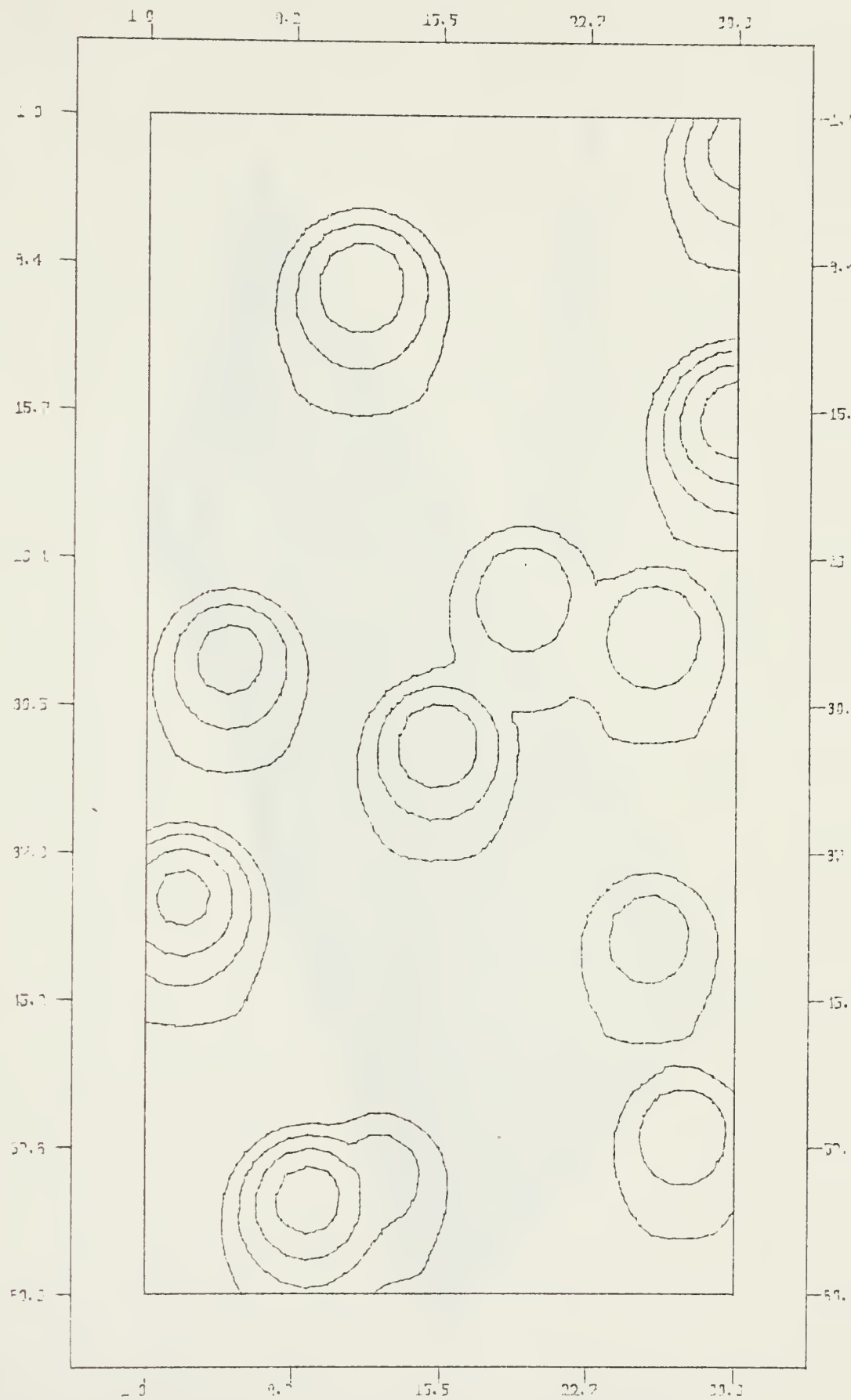


FIGURE 14-2. Terrain: 2, # of Hills; 12, Average Height; 100, Slope; Up

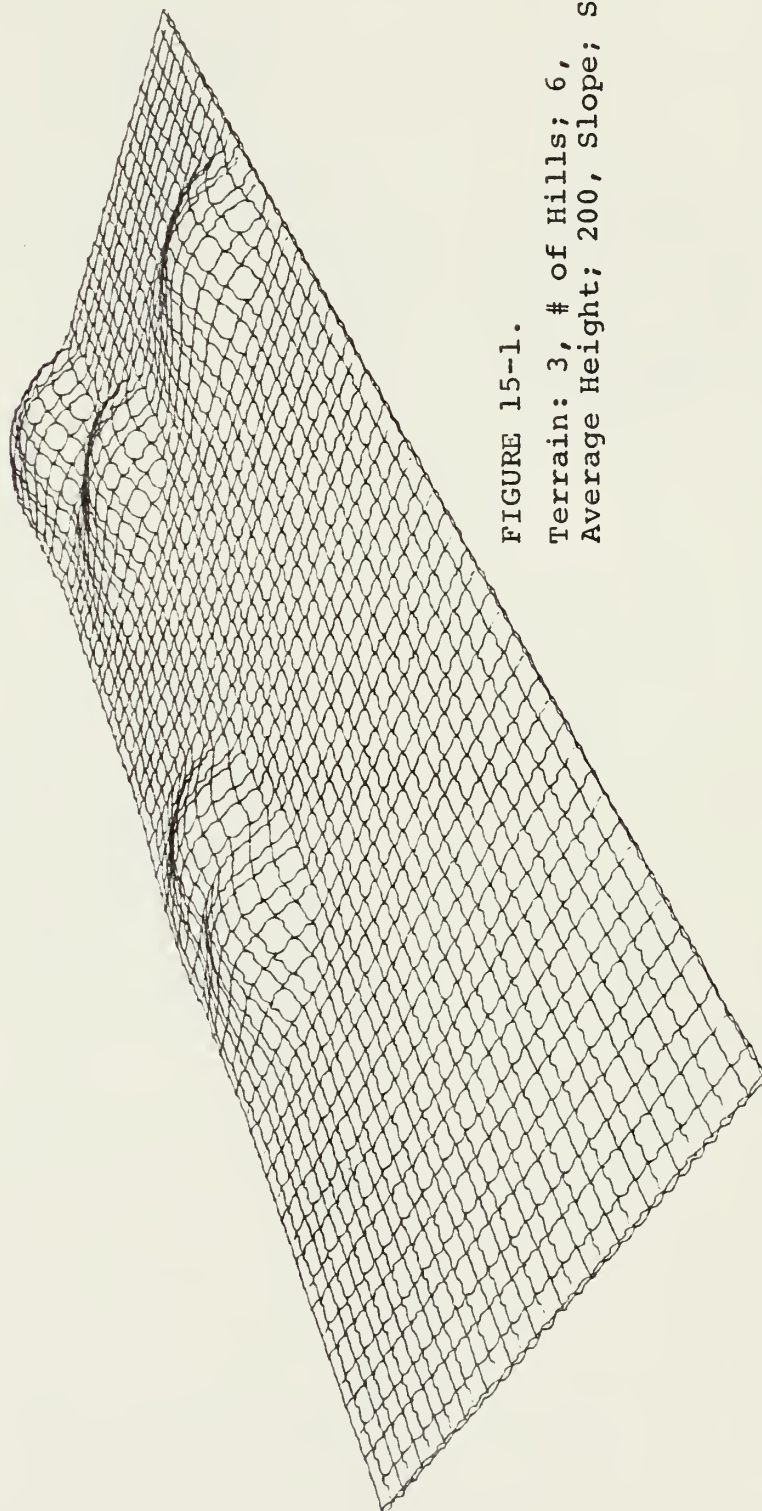


FIGURE 15-1.

Terrain: 3, # of Hills; 6,
Average Height; 200, Slope; Side

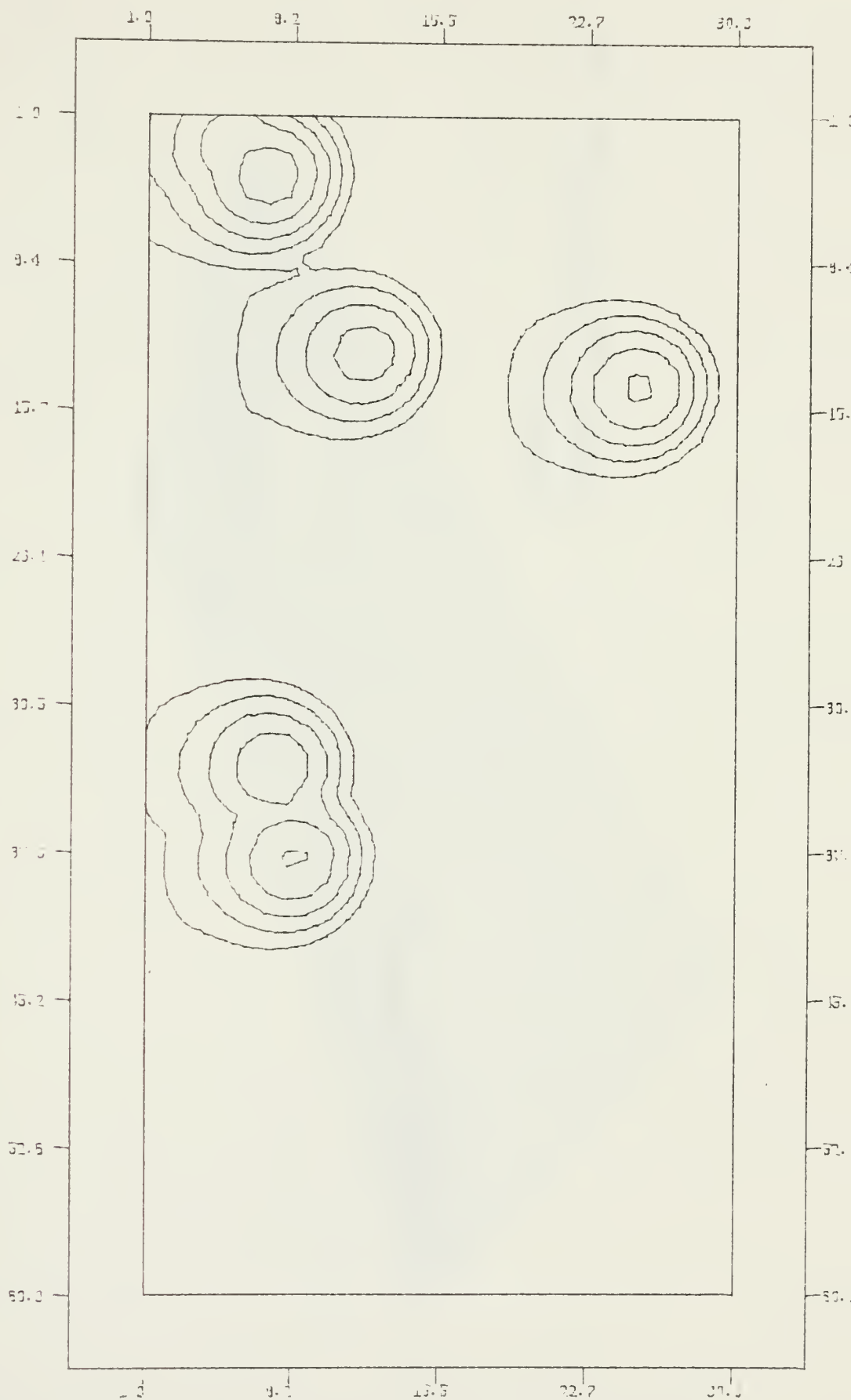


FIGURE 15-2. Terrain: 3, # of Hills: 6, Average Height;
200, Slope; Side

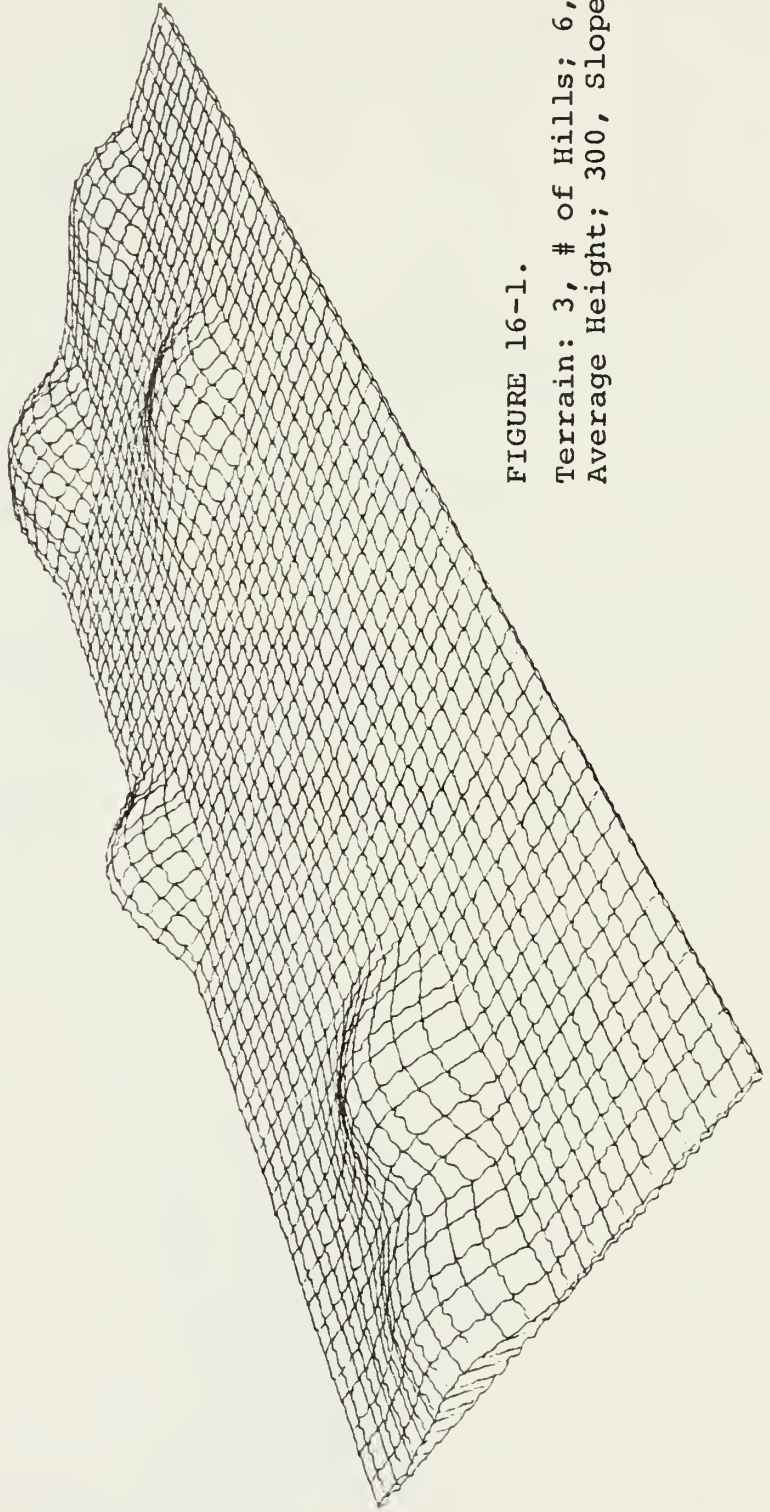


FIGURE 16-1.

Terrain: 3, # of Hills; 6,
Average Height; 300, Slope; side

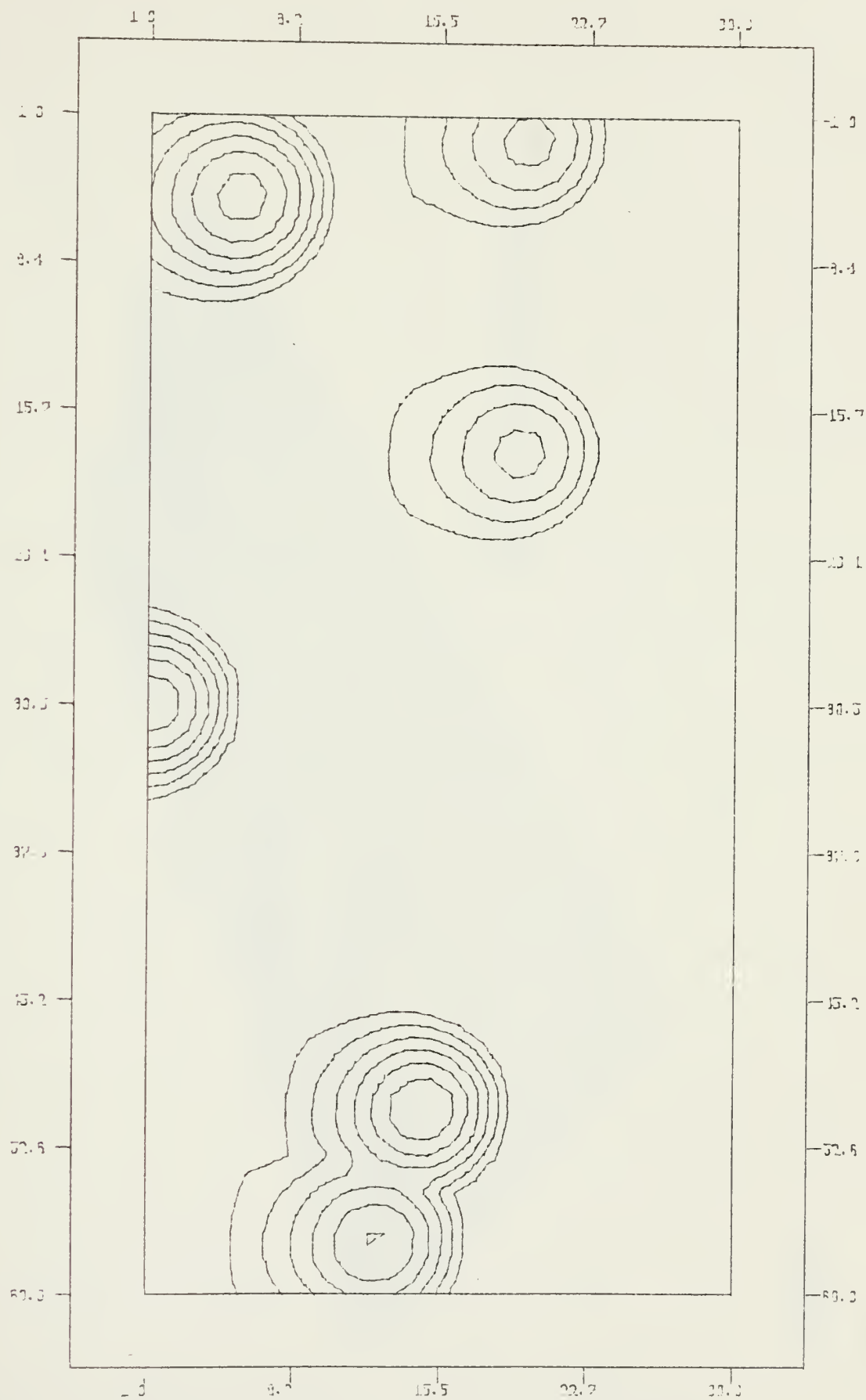


FIGURE 16-2. Terrain: 3, # of Hills; 6, Average Height; 300, Slope; Side.

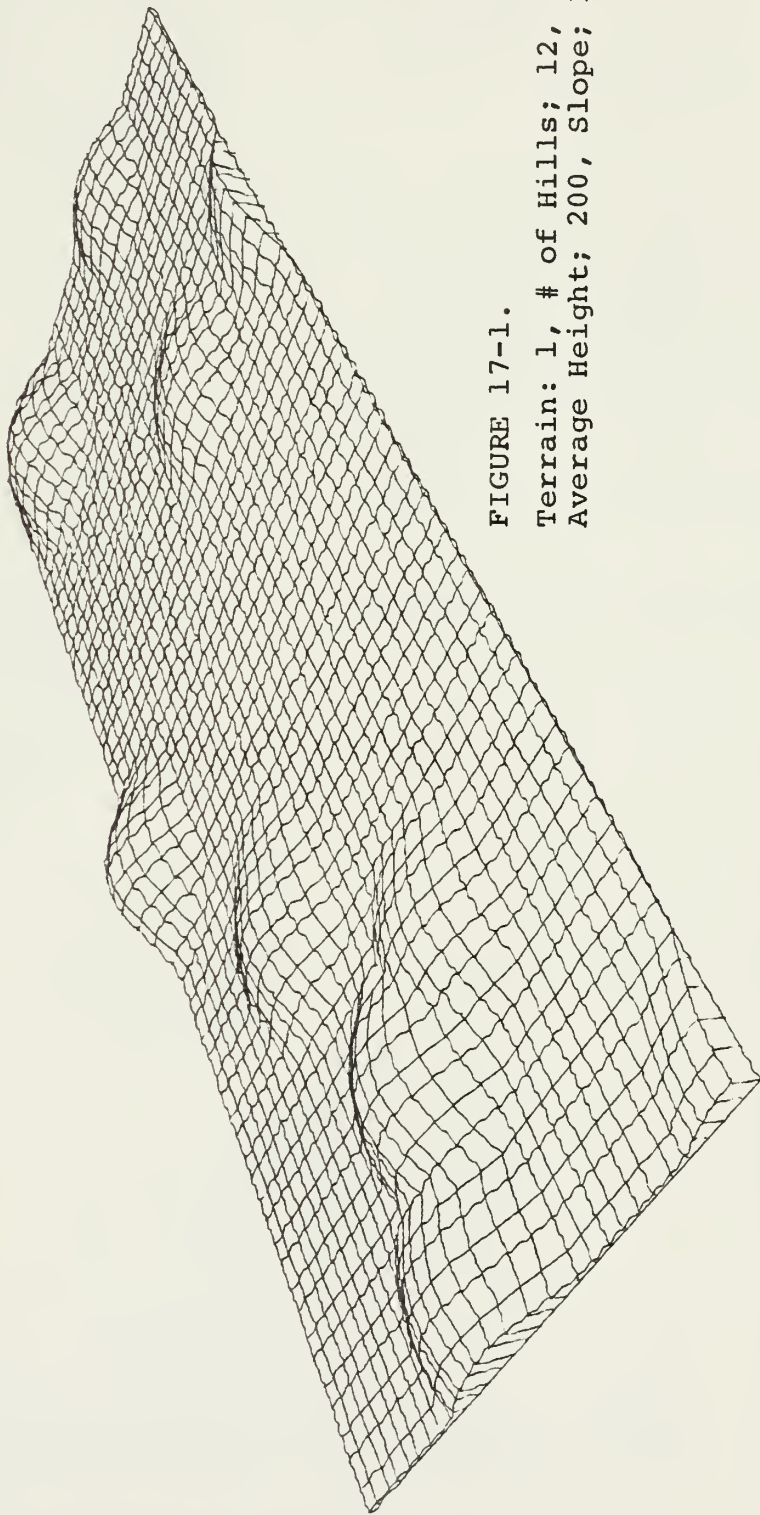


FIGURE 17-1.
Terrain: 1, # of Hills; 12,
Average Height; 200, Slope; Both

1 2 3 4 5 6 7 8 9 10 11 12

TERRAIN

2
1
X

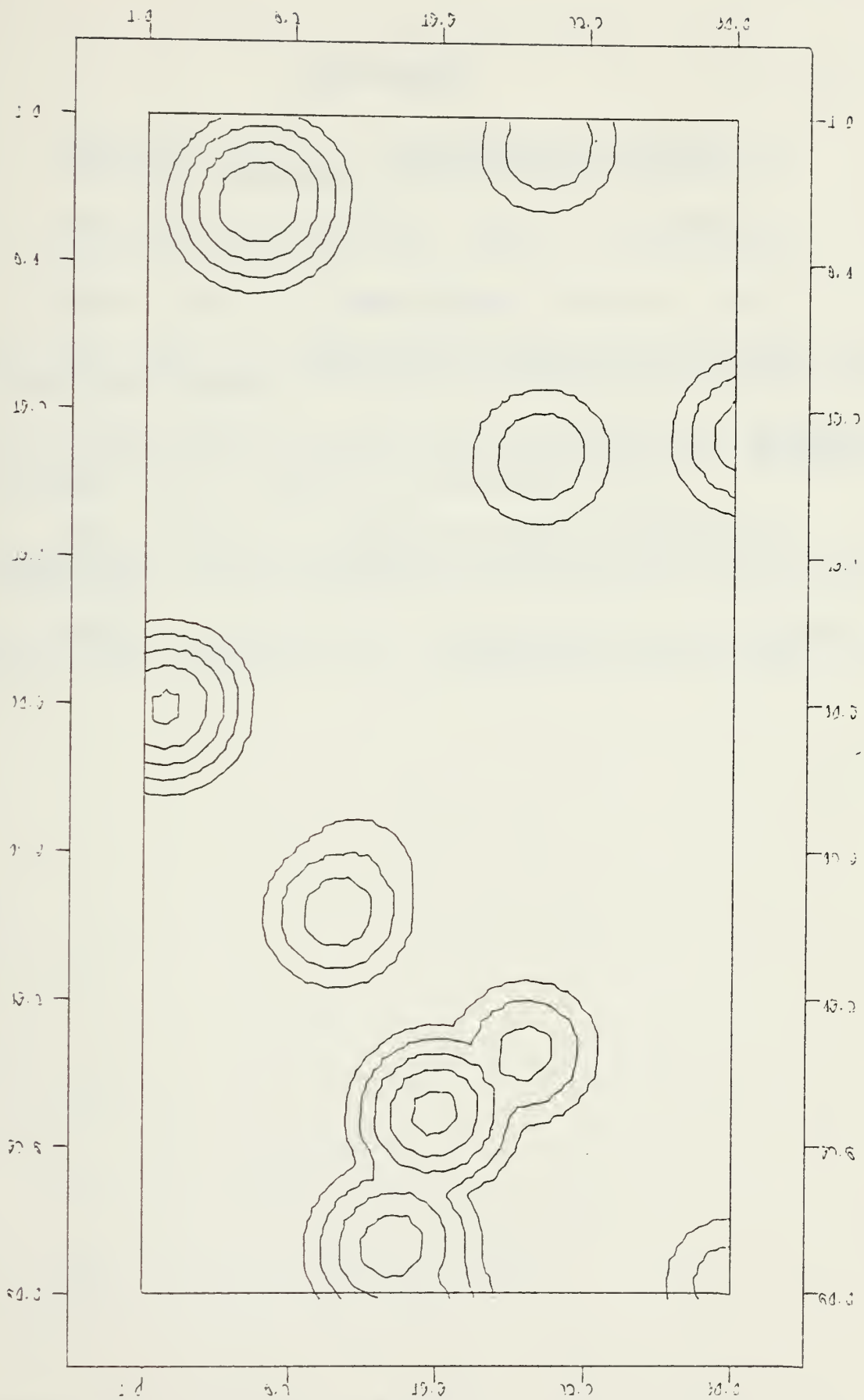


FIGURE 17-2. Terrain: 1, # of Hills; 12, Average Height; 200, Slope; Both

BIBLIOGRAPHY

1. Luenberger, David G., Introduction to Linear and Nonlinear Programming, Addison-Wesley, 1973.
2. Barr, Donald R. and Zehna, Peter W., Probability, Brooks/Cole Publishing Co., 1971.
3. Searle, Shale R., Linear Models, Wiley Co., 1971.
4. Kirk, Rober E., Experimental Design Procedures for the Behavioral Sciences, Brooks/Cole Publishing Co., 1968.
5. Farrell, Robert L., and Freedman, Richard J., Investigation of the Variation of Combat Model Predictions with Terrain Line of Sight, Vector Research Incorporated, 1975.
6. Raney, Sharon D., Three-Dimensional Isometric or Perspective Off-Line Plotting Sub-Program with Hidden-Line Elimination, Naval Postgraduate School, 1974.
7. Needels, Christopher J., Parameterization of Terrain in Army Combat Analysis, Naval Postgraduate School, 1976.

INITIAL DISTRIBUTION LIST

	No. Copies
1. Defense Documentation Center Cameron Station Alexandria, Virginia 22314	2
2. Library, Code 0212 Naval Postgraduate School Monterey, California 93940	2
3. Department Chairman, Code 55 Department of Operations Research Naval Postgraduate School Monterey, California 93940	1
4. Professor Samuel H. Parry, Code 55Py Department of Operations Research Naval Postgraduate School Monterey, California 93940	2
5. MAJ Christopher J. Needels 76-77CGSO Regular Course Fort Leavenworth, Kansas 66027	1
6. Vector Research, Incorporated ATTN: Mr. Robert Farrell P.O. Box 1506 Ann Arbor, Michigan 48106	1
7. U.S. Army Armor and Engineer Board ATTN: ATZK-AE-TA Fort Knox, Kentucky 40121	1
8. Commander, U.S. Army Training and Doctrine Command ATCD-AO ATTN: Mr. James Smith Fort Monroe, Virginia 23651	1
9. Director, TRADOC Systems Analysis Activity ATAA-TEM ATTN: Mr. Carrol Denny Mr. Al Burnham White Sands Missile Range New Mexico 88002	1
10. BDM Scientific Support Laboratory ATTN: Dr. R.P. Marchi Fort Ord, California 93941	1

11. LTC Kim, Chung Young 1
373-9 Myon Mock Dong,
Dong Dae Moon Ku,
Seoul 130-01, KOREA
12. OR Department 1
Deputy Chief of Staff for
Plan and Administration
ROKA HQ, Seoul, KOREA
13. OR Department 1
Deputy Chief of Staff for
Operation
ROKA HQ, Seoul, KOREA

Thesis

169902

K4145 Kim

c.1

Generation and analysis of parameterized terrain for land combat.

29 OCT 82

26190

28173

Thesis

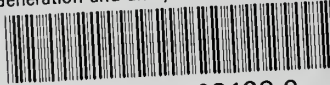
169902

K4145 Kim

c.1

Generation and analysis of parameterized terrain for land combat.

Generation and analysis of parameterized



3 2768 001 03128 9

DUDLEY KNOX LIBRARY